Delft University of Technology

Delft Center for Systems and Control

Technical report 03-008

Structural properties of Helbing's traffic flow model*

I. Necoara, B. De Schutter, and J. Hellendoorn

If you want to cite this report, please use the following reference instead:
I. Necoara, B. De Schutter, and J. Hellendoorn, "Structural properties of Helbing's traffic flow model," *Proceedings of the 83rd Annual Meeting of the Transportation Research Board*, Washington, DC, 22 pp., Jan. 2004. Paper 04-2263.

Delft Center for Systems and Control
Delft University of Technology
Mekelweg 2, 2628 CD Delft
The Netherlands
phone: +31-15-278.24.73 (secretary)
URL: `https://www.dcsc.tudelft.nl`

*This report can also be downloaded via `https://pub.deschutter.info/abs/03_008.html`

Structural Properties of Helbing's Traffic Flow Model

Authors:
I. Necoara, Delft Center for Systems and Control, Delft University of Technology, Mekelweg 2, 2628 CD Delft, The Netherlands, phone: +31-15-278.71.71, fax:+31-15-278.66.79, i.necoara@dcsc.tudelft.nl

B. De Schutter (corresponding author), Delft Center for Systems and Control, Delft University of Technology, Mekelweg 2, 2628 CD Delft, The Netherlands, phone: +31-15-278.51.13, fax: +31-15-278.66.79, b.deschutter@dcsc.tudelft.nl

J. Hellendoorn, Delft Center for Systems and Control, Delft University of Technology, Mekelweg 2, 2628 CD Delft, The Netherlands, phone: +31-15-278.90.07, fax: +31-15-278.66.79, j.hellendoorn@dcsc.tudelft.nl

Abstract. This paper analyzes the structural properties of the shock and rarefaction wave solutions of a macroscopic, second-order non-local continuum traffic flow model, namely Helbing's model. We will show that this model has two families of characteristics for the shock wave solutions: one characteristic is slower, and the other one is faster than the average vehicle speed. Corresponding to the slower characteristic we have 1-shocks and 1-rarefaction waves, the behavior of which is similar to that of shocks and rarefaction waves in the first-order model of Lighthill-Whitham-Richards. Corresponding to the faster characteristic there are 2-shocks and 2-rarefaction waves, which behave differently from the previous one, in the sense that the information in principle travels faster than average vehicle speed, but — as we shall see — in Helbing's model this inconsistency is solved via the addition of a non-local term. We will show that for the Helbing model the shocks do not produce negative states as other second-order models do. In this paper we also derive the formulas for the solution of the Riemann problem associated with this model in the equilibrium case.

1 INTRODUCTION

Many researchers consider that traffic behavior on a freeway at a given point in time-space is only affected by the conditions of traffic in a neighborhood of that point, proposing different models based on partial differential equations. In this context, one of the most well known traffic flow models is the Lighthill-Whitham-Richards (LWR) model (*12, 17, 19*), which is a first-order model. Whitham (*19*) and Payne (*15*) came up with a second-order traffic model. In this paper we discuss yet another macroscopic second-order model, which is based on gas-kinetic equations with a non-local term as proposed by Helbing (*4, 6, 7*) (see also (*9*)). In this model traffic is described macroscopically as if it were a fluid with the cars as molecules, obtaining the traffic equations from a gas-kinetic level of description. Helbing derived a model by applying statistical kinetic theory, where macroscopic laws are obtained from integration of molecular properties such as positions, collisions, overtaking, and velocities.

As an introduction to our discussion and to make the paper self-contained, a brief review of the Helbing model is presented. The new contributions of this paper start with Section 2, where we discuss the structural properties of the shock wave solution. In Section 3 we present the structural properties of the rarefaction waves solution, and in Section 4 we discuss the solution of the Riemann problem associated with the Helbing model. The detailed derivation of the formulas for the shock and rarefaction waves is given in Section 5. Finally, in Section 6 we discuss some possible future research directions.

In general, continuum macroscopic traffic models contain two independent variables: location x, and time t. There usually are three state variables: density ρ, average speed V, and flow Q with $Q = \rho V$. Because the number of vehicles is conserved, all macroscopic traffic flow models are based on the continuity equation, which expresses the relation between the rates of change of the density $\rho(x,t)$ w.r.t. t and of the flow $Q(x,t)$ w.r.t. x:

$$\frac{\partial \rho}{\partial t} + \frac{\partial Q}{\partial x} = 0 \ .$$

To describe time-varying and spatially varying average velocities $V(x,t)$ such as those that occur in traffic jams or stop-and-go traffic we need a dynamic velocity equation. Gas-kinetic equations for the average velocity have been proposed in a number of publications such as the papers by Prigogine and Herman (*16*), Paveri-Fontana (*14*), and Hoogendoorn and Bovy (*8*). Because we are interested in macroscopic quantities we can integrate those equations to derive formulas for the first moment. For all these models after integration, the equation for average velocity can be written as

$$\frac{\partial V}{\partial t} + V\frac{\partial V}{\partial x} + \frac{1}{\rho}\frac{\partial P}{\partial x} = \frac{V_{\rm e} - V}{\tau} \ ,$$

where P is the traffic pressure, defined as $P(x,t) = \rho(x,y)\theta(x,t)$ with θ the velocity variance (see also equation (2) below), and where $V_{\rm e}$ is the dynamical equilibrium velocity towards which the average velocity of vehicles relaxes. Helbing derived macroscopic traffic equations using the gas-kinetic traffic equations of Paveri-Fontana and a method analogous to the derivation of the Euler equations for ordinary fluids (i.e., the Chapman-Enskog expansion). Compared to the other models, in the Helbing model the dynamical equilibrium velocity $V_{\rm e}$ also depends on the density and average velocity at an interaction point that is advanced by about the safe distance. More specifically, Helbing proposes the following Euler-like equation with a non-local term for the average vehicle velocity:

$$\frac{\partial V}{\partial t} + \underbrace{V\frac{\partial V}{\partial x}}_{\text{transport}} + \underbrace{\frac{1}{\rho}\frac{\partial P}{\partial x}}_{\text{pressure}} = \underbrace{\frac{V_0 - V}{\tau}}_{\text{acceleration}} \underbrace{- \frac{V_0(\theta + \theta_{\rm a})}{\tau A(\rho_{\max})}\left(\frac{\rho_{\rm a} T}{1 - \rho_{\rm a}/\rho_{\max}}\right)^2 B(\delta_{\rm v})}_{\text{braking}} \ . \tag{1}$$

So, the change in time of the average velocity V is given by: a *transport term* originating from the propagation of the velocity profile with the average velocity V, a *pressure term* that has a dispersion effect

due to a finite variance of the vehicle velocities, an *acceleration term* describing the acceleration towards the average desired velocity V_0 of the drivers with relaxation time τ, and finally a *braking term*: this is a non-local term that models braking in response to traffic situation downstream at the interaction point $x_{\rm a} = x + \gamma(1/\rho_{\max} + TV)$ with $1 < \gamma < 2$ a model parameter, $\rho_{\max}$ is the maximum density, and T is the average time headway. In equation (1) we also have a Boltzmann factor of the form

$$B(\delta_{\rm v}, S) = \delta_{\rm v} \frac{e^{-z^2/2}}{\sqrt{2\pi}} + (1 + \delta_{\rm v}^2) \int_{-\infty}^{\delta_{\rm v}} \frac{e^{-z^2/2}}{\sqrt{2\pi}}\, dz \ ,$$

with $\delta_{\rm v} = \frac{V - V_{\rm a}}{\sqrt{\theta - \theta_{\rm a}}}$, which takes into account the velocity and variance at the actual position x and the interaction point $x_{\rm a}$ respectively. This non-local term around location $x_{\rm a}$ expresses that interactions between vehicles are forwardly directed, since drivers mainly react to the traffic situation in front of them until a certain distance. In this way Helbing remedies an inconsistency of previous models that was criticized by Daganzo (*2*), namely that although the fluid particles respond to stimuli from ahead and from behind, a car is an anisotropic particle that responds to frontal stimuli (i.e., we require an anisotropic model). The shift term $d = \gamma(1/\rho_{\max} + TV)$ is taken from a car-following model and expresses the velocity-dependent safe distance. Based on empirical data Helbing observed that the velocity variance θ (which appears in the definition of the traffic pressure $P = \rho\theta$) is a density-dependent fraction $A(\rho)$ of the squared velocity:

$$\theta(x,t) = A(\rho(x,t)) V^2(x,t) \ , \tag{2}$$

where $A(\rho)$ is the Fermi function:

$$A(\rho) = A_0 + \Delta A \left(1 + \tanh\left(\frac{\rho - \rho_{\rm c}}{\Delta\rho}\right)\right) \ , \tag{3}$$

where A_0 and $A_0 + 2\Delta A$ are about the variance factors for free and congested traffic, $\rho_{\rm c}$ is of the order of the critical density for the transition from free to congested traffic, and $\Delta\rho$ is the width of the transition.

To summarize, the equations of Helbing's model are:

$$\frac{\partial \rho}{\partial t} + \frac{\partial Q}{\partial x} = 0 \tag{4}$$

$$\frac{\partial V}{\partial t} + V\frac{\partial V}{\partial x} + \frac{1}{\rho}\frac{\partial P}{\partial x} = \frac{V_{\rm e} - V}{\tau} \tag{5}$$

$$Q = \rho\, V \ , \tag{6}$$

where the equilibrium velocity is written as

$$V_{\rm e} = V_0 \left(1 - \frac{\theta + \theta_{\rm a}}{A(\rho_{\max})} \left(\frac{\rho_{\rm a} T}{1 - \rho_{\rm a}/\rho_{\max}}\right)^2 B(\delta_{\rm v})\right) \ . \tag{7}$$

Readers interested in an empirical validation of this model are referred to (*5*).

2 HUGONIOT LOCUS AND SHOCKS

In this section we show that the Helbing model can be written in a conservative form, and then we study the shocks arising from this model and we derive conditions under which a pair of states can be connected by a shock (i.e., we determine the Hugoniot locus). We will show that the shocks do not produce negative states

as other second-order models do (see (*2*)). Therefore, for this model the Riemann problem is physically well-posed (see also Section 4).

Using $Q = \rho V$ and $P = \rho\theta = \rho A(\rho)V^2$, we can write

$$\rho V^2 + P = \frac{Q^2}{\rho}(1 + A(\rho)) \ .$$

Then using previous formulas we see that a desirable property of the Helbing model equations (4)–(7) is that they can be formulated in terms of a system of *conservation equations* (i.e., a time-dependent system of nonlinear partial differential equations with a particular simple structure) but with a source term:

$$\frac{\partial u}{\partial t} + \frac{\partial f(u)}{\partial x} = S(u) \tag{8}$$

with state variables

$$u = \begin{bmatrix} \rho \\ Q \end{bmatrix} \ ,$$

flux function

$$f(u) = \begin{bmatrix} Q \\ \frac{Q^2}{\rho}(1 + A(\rho)) \end{bmatrix} \ ,$$

and source term

$$S(u) = \begin{bmatrix} 0 \\ \frac{\rho V_{\mathrm{e}} - Q}{\tau} \end{bmatrix} \ .$$

In matrix representation using the Jacobian $J(u) \stackrel{\text{def}}{=} \frac{\partial f(u)}{\partial u}$ we have

$$\frac{\partial}{\partial t}\begin{bmatrix} \rho \\ Q \end{bmatrix} + \underbrace{\begin{bmatrix} 0 & 1 \\ -\frac{Q^2}{\rho^2} + \frac{\partial P}{\partial \rho} & 2\frac{Q}{\rho} + \frac{\partial P}{\partial Q} \end{bmatrix}}_{J(u)} \cdot \frac{\partial}{\partial x}\begin{bmatrix} \rho \\ Q \end{bmatrix} = \begin{bmatrix} 0 \\ \frac{\rho V_{\mathrm{e}} - Q}{\tau} \end{bmatrix} \ .$$

In our case pressure has the form $P = \rho A(\rho)V^2 = \frac{Q^2}{\rho}A(\rho)$, which implies that

$$J(u) = \begin{bmatrix} 0 & 1 \\ -\frac{Q^2}{\rho^2}(1 + A(\rho) - \rho\frac{d}{d\rho}A(\rho)) & 2\frac{Q}{\rho}(1 + A(\rho)) \end{bmatrix} \ .$$

When we compute the eigenvalues of the Jacobian, and using again the relation $V = \frac{Q}{\rho}$, we get

$$\lambda_{1,2}(u) = V\left(1 + A(\rho) \pm \sqrt{A^2(\rho) + A(\rho) + \rho\frac{d}{d\rho}A(\rho)}\right) \ . \tag{9}$$

Using the fact that $A(\cdot)$ is a Fermi function, it can be proved that for physical values of ρ the radical in (9) is well-defined, and that the eigenvalues are real and distinct. We see that λ_1 is smaller than the average vehicle velocity V, but λ_2 is larger than V. This is a drawback of this kind of models because this means that information travels faster than average vehicles speed, which was criticized by del Castillo (*3*) and Daganzo (*2*). However, note that V is an average vehicle speed, so there may exist vehicles that travel faster or slower than V.

Corresponding to the two distinct eigenvalues given by equation (9) we have two linearly independent eigenvectors

$$r_{1,2}(u) = \begin{bmatrix} 1 \\ \lambda_{1,2}(u) \end{bmatrix} \ .$$

Assumption A1: As Helbing recommends in (*6*) for qualitative considerations, $A(\rho)$ can be chosen to be constant. We adopt this assumption henceforth because it simplifies our computations. We choose for $A(\rho)$ the value $c \stackrel{\text{def}}{=} A_0 + \Delta A \approx 0.028$ (which is the value around critical density where we have large oscillations of the speed).

With Assumption A1 the formulas for pressure P, flux f, and the eigenvalues λ_p ($p = 1, 2$) are

$$\begin{aligned} P &= c\rho V^2 = c\frac{Q^2}{\rho} \\ f(u) &= \begin{bmatrix} Q \\ \frac{Q^2}{\rho}(1+c) \end{bmatrix} \\ \lambda_{1,2}(u) &= V\left(1 + c \pm \sqrt{c^2 + c}\right) = c_{1,2}V \ , \end{aligned}$$

where we denote $c_1 \stackrel{\text{def}}{=} 1 + c - \sqrt{c^2 + c} \in (0,\ 1)$ and $c_2 \stackrel{\text{def}}{=} 1 + c + \sqrt{c^2 + c} > 1$. Note that $\lambda_1 < \lambda_2$. Using the weak formulation (*11*) we can expand the class of solutions of the hyperbolic system (8) so as to include discontinuous solutions called *shocks*. Now let us study different kinds of shocks arising from the system and determine and characterize the conditions under which a pair of states $\hat{u} = [\hat{\rho} \quad \hat{Q}]^T$, $\tilde{u} = [\tilde{\rho} \quad \tilde{Q}]^T$ can be connected by a single shock.

First, note that in *short* time intervals the shocks arising from (8) are the same as those arising from

$$\frac{\partial}{\partial t}\begin{bmatrix} \rho \\ Q \end{bmatrix} + \begin{bmatrix} 0 & 1 \\ -\frac{Q^2}{\rho^2}(1+c) & 2\frac{Q}{\rho}(1+c) \end{bmatrix} \cdot \frac{\partial}{\partial x}\begin{bmatrix} \rho \\ Q \end{bmatrix} = 0 \ , \tag{10}$$

i.e., the source term becomes zero (this can be done when traffic operations are in equilibrium but also because the relaxation term $\frac{\rho V_e - Q}{\tau}$ is finite, so that its effect in short time intervals can be neglected in comparison with the effect caused by the infinite space derivatives of ρ and Q at the shock).

Because we have two characteristics (eigenvalues), two kinds of shocks arise from (10): we call them *1-shock* and *2-shock* respectively. Let us fix a state $\hat{u} = [\hat{\rho} \quad \hat{Q}]^T$, and determine the set of states $\tilde{u}$ that can be connected by a discontinuity (called *Hugoniot locus*) to the point $\hat{u}$. For this, the Rankine-Hugoniot jump condition (*11*) must hold:

$$f(\tilde{u}) - f(\hat{u}) = s \cdot (\tilde{u} - \hat{u}) \ , \tag{11}$$

where s is the propagation speed of the discontinuity along the road (known in traffic flow engineering as *congestion velocity*). The condition (11) expresses the fact that the propagation of a shock depends on both flow and density in the neighboring (upstream and downstream) region of a shock.

Furthermore, we should also take into account whether a given discontinuity is physically relevant. To this extent Lax (*10*) proposed an entropy condition: the jump in the pth field (from state $\hat{u}$ to $\tilde{u}$) is admissible only if

$$\lambda_p(\hat{u}) > s > \lambda_p(\tilde{u}) \ .$$

After some computations this results in the following conditions for a 1-shock (see Section 5.1 for details):

$$\text{S1}: \quad \tilde{Q} = \hat{Q}\frac{1-(\tilde{\rho}-\hat{\rho})\sqrt{\frac{c^2+c}{\tilde{\rho}\hat{\rho}}}}{1-\frac{\tilde{\rho}-\hat{\rho}}{\tilde{\rho}}(1+c)}, \quad \tilde{\rho} > \hat{\rho}, \quad \tilde{Q} > \hat{Q} \tag{12}$$

with the corresponding speed of propagation

$$s_1 = \hat{Q}\frac{\frac{1+c}{\tilde{\rho}} - \sqrt{\frac{c^2+c}{\tilde{\rho}\hat{\rho}}}}{1-\frac{\tilde{\rho}-\hat{\rho}}{\tilde{\rho}}(1+c)} \ . \tag{13}$$

Now let us see what the interpretation is of a 1-shock. Do the drivers on the average really behave as described by S1 in (12)? If we consider the *fundamental diagram* that relates speed and density then we see that the condition $\tilde{\rho} > \hat{\rho}$ implies that $\tilde{V} < \hat{V}$, i.e., the drivers that enter that shock reduce their speed abruptly, which coincides with real-life behavior (see also (*1*)).

In a similar way as for the 1-shock we can show that for a 2-shock we have

$$\text{S2}: \quad \tilde{Q} = \hat{Q}\frac{1+(\tilde{\rho}-\hat{\rho})\sqrt{\frac{c^2+c}{\tilde{\rho}\hat{\rho}}}}{1-\frac{\tilde{\rho}-\hat{\rho}}{\tilde{\rho}}(1+c)}, \quad \tilde{\rho} < \hat{\rho}, \quad \tilde{Q} < \hat{Q}$$

and the corresponding speed of propagation

$$s_2 = \hat{Q}\frac{\frac{1+c}{\tilde{\rho}} + \sqrt{\frac{c^2+c}{\tilde{\rho}\hat{\rho}}}}{1-\frac{\tilde{\rho}-\hat{\rho}}{\tilde{\rho}}(1+c)} \ .$$

Let us now study the sign for the propagation speeds s_1 and s_2 of the discontinuity. We distinguish two cases:

1. If the denominator $1-\frac{\tilde{\rho}-\hat{\rho}}{\tilde{\rho}}(1+c)$ is larger than 0, then $\tilde{\rho} < \hat{\rho}(1+\frac{1}{c})$, and we obtain that $0 < s_1 < s_2$, i.e., the speed of propagation of the 1-shock is less than the speed of the 2-shock, but both are positive, i.e., the discontinuity moves downstream.

2. If the denominator is less than 0, then $\tilde{\rho} > \hat{\rho}(1+\frac{1}{c})$ and $s_2 < 0 < s_1$, i.e., the speed for the 1-shock is positive and it moves downstream, but the speed for the 2-shock is negative, and it moves upstream.

Now we can sketch the Hugoniot locus in the phase plane, retaining only the points $\tilde{u}$ that can be connected to $\hat{u}$ by an entropy-satisfying shock, discarding the entropy-violating shocks (dotted lines in Figure 1). Any right state $u_\text{r} = [\rho_\text{r} \ \ Q_\text{r}]^T$ can be connected to a left state $u_\text{l} = [\rho_\text{l} \ \ Q_\text{l}]^T$ by a 1-shock if the right state falls on the S1 curve that passes through $[\rho_\text{l} \ \ Q_\text{l}]^T$ and similarly by a 2-shock if the right state falls on the S2 curve that passes through $[\rho_\text{l} \ \ Q_\text{l}]^T$. We can see from Figure 1 that the Hugoniot locus terminates at the origin and there are no states with $u_\text{r} < 0$ that can be connected to u_l by a propagating discontinuity; therefore, the model does not produce negative density and flow at the point of discontinuity (as others models that do so, see Daganzo (*2*) for details), so it makes physical sense to discuss about Riemann problem associated with this model (as we will do in Section 4).

3 RAREFACTION WAVES

For the LWR model it is known that when the left characteristic is slower than the right characteristic a fan of rarefaction waves results. In this section we show that Helbing's model also has this property, deriving

the rarefaction curves corresponding to this model. We will see again that we cannot connect negative states through this kind of rarefaction waves. We will use this result when we discuss about Riemann problem.

If the two characteristic fields satisfy

$$\lambda_p(u_\mathrm{l}) < \lambda_p(u_\mathrm{r}) \quad \text{for } p = 1, 2\,, \tag{14}$$

two families of smooth solutions, called *1-rarefaction waves* and *2-rarefaction waves* exist. Similar to the analysis of shock curves we shall derive the phase curves for both families of rarefaction waves. One can write (10) as:

$$\frac{\partial u}{\partial t} + J(u)\frac{\partial u}{\partial x} = 0 \quad \text{with } u = [\rho \;\; Q]^T,\;\; f = \left[Q \;\; \frac{Q^2}{\rho}(1+c)\right]^T,\;\; J(u) = \frac{\partial f}{\partial u}\;. \tag{15}$$

If $u(x,t)$ is a solution of the system (15), then we can show that $u(ax, at)$ is also a solution, where a is a scalar, i.e., the solutions are scaling-invariant. Therefore, the solution depends on (x,t) in the form $\xi = x/t$. A rarefaction wave solution to the system of equations takes the form:

$$u(x,t) = \begin{cases} u_\mathrm{l} & \text{if} \;\; x \le \xi_1 t \\ w(x/t) & \text{if} \;\; \xi_1 t < x < \xi_2 t \\ u_\mathrm{r} & \text{if} \;\; x \ge \xi_2 t\,, \end{cases} \tag{16}$$

with $w(\cdot)$ smooth and $w(\xi_1) = u_\mathrm{l}$ and $w(\xi_2) = u_\mathrm{r}$. We will now prove that starting at each point u_l there are two curves consisting of points u_r that can be connected to u_l by a rarefaction wave, namely a subset of the integral curve of $r_p(u_\mathrm{l})$. An integral curve for $r_p(u)$ is a curve that has the property that the tangent to the curve at any point u lies in the direction $r_p(u)$. In order to determine explicitly the function $w(x/t)$ we differentiate $u(x,t) = w(x/t)$:

$$\begin{aligned} \frac{\partial u}{\partial t}(x,t) &= -\frac{x}{t^2}w'(x/t) \\ \frac{\partial u}{\partial x}(x,t) &= \frac{1}{t}w'(x/t)\;\;, \end{aligned}$$

where $w'(\cdot)$ represents the derivative of $w(\cdot)$. Replacing these expressions in (15) with $\xi = x/t$ we get

$$J(w(\xi)) \cdot w'(\xi) = \xi w'(\xi)\;\;, \tag{17}$$

which means that $w'(\xi)$ is proportional to some eigenvector $r_p(w(\xi))$ of the Jacobian $J(w(\xi))$:

$$w'(\xi) = \alpha(\xi) \cdot r_p(w(\xi))\;\;,$$

i.e., $w(\xi)$ lies along some integral curve of r_p and ξ is an eigenvalue of the Jacobian.

Computing $w(\cdot)$ results in the following expression for the 1-rarefaction curve (see Section 5.2 for details):

$$\text{R1}: \quad Q_\mathrm{r} = Q_\mathrm{l}\left(\frac{\rho_\mathrm{r}}{\rho_\mathrm{l}}\right)^{c_1}, \quad \rho_\mathrm{r} < \rho_\mathrm{l}\;. \tag{18}$$

The 2-rarefaction curve is given by

$$\text{R2}: \quad Q_\mathrm{r} = Q_\mathrm{l}\left(\frac{\rho_\mathrm{r}}{\rho_\mathrm{l}}\right)^{c_2}, \quad \rho_\mathrm{r} > \rho_\mathrm{l}\;. \tag{19}$$

Figure 2 shows the states u_{r} that can be connected to u_{l} by a 1-rarefaction wave, namely the states lying on the curve R1 passing through u_{l}. Furthermore, the states u_{r} lying on the curve R2 passing through u_{l} can be connected to u_{l} by a 2-rarefaction wave. We can observe that the integral curves R1 and R2 are very similar to the Hugoniot locus. Moreover, locally near the point u_{l} they must be in fact very close to each other, because each of these curves is tangent to $r_p(u_{\mathrm{l}})$ at u_{l}. Therefore, locally around u_{l} the rarefaction waves are similar with the shock waves (we can see that a 1-rarefaction wave is similar to a 2-shock wave, and that a 2-rarefaction is similar to a 1-shock wave). Note that this does not imply non-existence of rarefaction wave solutions for the Helbing model, because this similarity is valid only locally and when we solve Riemann problem the intermediate states u_{m} can be given by the intersection of a shock curve with a rarefaction curve (see also Section 4). Again we see that we do not connect negative states to u_{l}, which is a very important feature of the Helbing model, and we will use this result when we discuss the Riemann problem. An interpretation in terms of driver behavior of the rarefaction waves is similar with that of entropy-satisfying shock.

4 GENERAL SOLUTION OF THE RIEMANN PROBLEM

In this section we discuss the Riemann problem associated with the Helbing model, and based on the results of the two previous sections we will show that solutions of the Riemann problem with density and flow non-negative in the initial condition on either side of the discontinuity cannot give rise to negative flows or densities later on. Also we will see that for Riemann problem we can find more than one solution, and the condition for uniqueness is to select the entropy-satisfying weak solution, which results in a unique, physically valid solution. A similar derivation as the one of this paper but for another model can be found in (*20*).

A conservation law together with piecewise constant initial data having a single discontinuity results in a so-called *Riemann problem* (see (*11, 13, 18*) for more details). E.g., the system (15) with initial condition

$$u(x,0) = \begin{cases} u_{\mathrm{l}} & \text{if } x < 0 \\ u_{\mathrm{r}} & \text{if } x > 0\,, \end{cases}$$

where u_{l} and u_{r} are given constants, is a Riemann problem.

If we combine Figures 1 and 2 we obtain a plot that shows us all points u_{r} that can be connected to a given point u_{l} by an entropy-satisfying wave (see Figure 3 – top), either a shock wave or a rarefaction wave (u_{r} lies on one of the curves S1, S2, R1 or R2), and the states u_{l} that can be connected to a given u_{r} (see Figure 3 – bottom). Therefore, when initial data u_{l} and u_{r} both lay on these curves then this discontinuity simply propagates with speed $s = \frac{Q_{\mathrm{r}} - Q_{\mathrm{l}}}{\rho_{\mathrm{r}} - \rho_{\mathrm{l}}}$ along the road.

But what happens if u_{r} does not reside on one of those curves passing through u_{l}? To solve this question, just as in the linear case, we can attempt to find a way to split this jump as a sum of two jumps, across each of which the Rankine-Hugoniot condition holds, i.e., we must find an intermediate state u_{m} such that u_{l} and u_{m} are connected by a discontinuity satisfying the Rankine-Hugoniot condition and so are u_{m} and u_{r}, which intuitively means to superimpose the appropriate plots and look for the intersections. When we want to determine analytically the intermediate state u_{m}, we must first determine whether each wave is a shock or a rarefaction, and then use the expressions relating ρ and Q determined in Sections 2 and 3 along each curve to solve for the intersection. When we solve the equation given by the intersection, we can get more than one solution for u_{m}, but only one gives a physically valid solution to the Riemann problem since the jump from u_{l} to u_{m} must travel more slowly than the jump from u_{m} to u_{r} (due to $\lambda_1 < \lambda_2$), therefore the condition for uniqueness is to pick up the weak solution that satisfies the above condition. Using the same parametrization $\rho_{\mathrm{l}} = \rho_{\mathrm{m}}(1+\xi_1)$ and $\rho_{\mathrm{r}} = \rho_{\mathrm{m}}(1+\xi_2)$, and replacing in (23) we get that the speeds of

shock from u_l to u_m and from u_m to u_r are given by:

$$s_{\mathrm{l,m}} = \frac{Q_\mathrm{m}}{\rho_\mathrm{m}} \frac{\frac{1+c}{1+\xi_1} \pm \sqrt{\frac{c^2+c}{1+\xi_1}}}{1-\frac{\xi_1(1+c)}{1+\xi_1}}, \quad s_{\mathrm{m,r}} = \frac{Q_\mathrm{m}}{\rho_\mathrm{m}} \frac{\frac{1+c}{1+\xi_2} \pm \sqrt{\frac{c^2+c}{1+\xi_2}}}{1-\frac{\xi_2(1+c)}{1+\xi_2}} .$$

Now depending on what values we choose for u_l and u_r we can determine the sign in the previous formulas such that $s_{\mathrm{l,m}} < s_{\mathrm{m,r}}$ and thus we know what waves (1-wave or 2-wave) give the intersection. We can distinguish the following cases:

Case 1: Both curves are shocks.

Graphically this means to draw the Hugoniot locus for each of the states u_l and u_r and to look for the intersection. To obtain the correct value for $u_\mathrm{m} = [\rho_\mathrm{m} \quad Q_\mathrm{m}]^T$ we have to impose $s_{\mathrm{l,m}} < s_{\mathrm{m,r}}$. Let us consider an example; e.g., assume that u_m is connected to u_l by a 1-shock and to u_r by a 2-shock:

$$Q_\mathrm{m} = Q_\mathrm{l} \frac{1-(\rho_\mathrm{m}-\rho_\mathrm{l})\sqrt{\frac{c^2+c}{\rho_\mathrm{m}\rho_\mathrm{l}}}}{1-\frac{\rho_\mathrm{m}-\rho_\mathrm{l}}{\rho_\mathrm{m}}(1+c)}, \quad Q_\mathrm{m} = Q_\mathrm{r} \frac{1+(\rho_\mathrm{m}-\rho_\mathrm{r})\sqrt{\frac{c^2+c}{\rho_\mathrm{m}\rho_\mathrm{r}}}}{1-\frac{\rho_\mathrm{m}-\rho_\mathrm{r}}{\rho_\mathrm{m}}(1+c)} . \tag{20}$$

Equating the two right-hand sides gives a single equation for ρ_m. If we set $y = \sqrt{\rho_\mathrm{m}}$, we get a 4th degree polynomial equation in y, which can either be solved analytically (using Ferrari's method) or numerically (using, e.g., Newton's method or Laguerre's algorithm). After we obtain ρ_m we replace it in one of the previous equalities (20) to obtain Q_m. Using a reasoning that is similar to the one of (*10*), it can be shown that the equation in ρ_m always has a solution when u_l and u_r are sufficiently close.

Case 2: Both curves are rarefactions.

If we assume that the intermediate state is connected to u_l by a 1-rarefaction and to u_r by a 2-rarefaction, then u_m must satisfy

$$Q_\mathrm{m} = Q_\mathrm{l} \left(\frac{\rho_\mathrm{m}}{\rho_\mathrm{l}}\right)^{c_1}, \quad Q_\mathrm{m} = Q_\mathrm{r} \left(\frac{\rho_\mathrm{m}}{\rho_\mathrm{r}}\right)^{c_2} . \tag{21}$$

Equating again we get an equation in ρ_m with solution

$$\rho_\mathrm{m} = \left(\frac{Q_\mathrm{l}}{Q_\mathrm{r}} \frac{\rho_\mathrm{r}^{c_2}}{\rho_\mathrm{l}^{c_1}}\right)^{\frac{1}{c_2-c_1}}$$

and then we obtain Q_m from (21). We proceed similarly when we consider the opposite case: u_m is connected to u_l by a 2-rarefaction and to u_r by a 1-rarefaction.

Case 3: The solution consist of one shock and one rarefaction wave.

Again if we consider the case when the intermediate state u_m is connected to u_l by a 1-rarefaction and to u_r by a 2-shock, then we must solve for ρ_m and Q_m from the equations:

$$Q_\mathrm{m} = Q_\mathrm{l} \frac{1+(\rho_\mathrm{m}-\rho_\mathrm{l})\sqrt{\frac{c^2+c}{\rho_\mathrm{m}\rho_\mathrm{l}}}}{1-\frac{\rho_\mathrm{m}-\rho_\mathrm{l}}{\rho_\mathrm{m}}(1+c)}, \quad Q_\mathrm{m} = Q_\mathrm{r} \left(\frac{\rho_\mathrm{m}}{\rho_\mathrm{r}}\right)^{c_1} .$$

We would like to point out that in general not for all u_l and u_r the weak solution previously constructed is a physically correct solution as it may be possible that one of the resulting shocks violate the entropy

condition. In particular, for any u_l the *feasible* (i.e., entropy-satisfying) u_r lie in a bounded region formed by horizontal axis (ρ) and the curves S1 and S2 (indicated by the hashed region in Figure 1).

Figure 4 shows a plot for the Riemann problem with initial conditions $u_\mathrm{l} = [140 \quad 400]^T$ and $u_\mathrm{r} = [5 \quad 50]^T$, which corresponds, e.g., to a scenario such as the situation of traffic in front of a semaphore when it was red and then becomes green. The full curves represent the states that can be connected to u_l, and the dotted curves represent the states that can be connected to u_r. The intersection gives two points: the intermediate state u_m is obtained by intersection of R1 with S2, and u^*_m by intersection of R2 with S1. So, the Riemann problem has more than one solution in this case (this happens also for other traffic flow models), but only one is a physically valid solution because we should have $s_{\mathrm{l,m}} < s_{\mathrm{m,r}}$ (due to $\lambda_1 < \lambda_2$). If we do the computations, we get that in this case u^*_m is the solution that satisfies the entropy condition, i.e., u^*_m is the physically valid solution.

5 DERIVATION OF THE WAVE FORMULAS

For the sake of completeness we now provide the details of the derivation of the formulas for the shock and rarefaction waves.

5.1 Derivation of the formulas for the shock waves

Consider the Rankine-Hugoniot jump condition (11). Filling out the expression for f results in the following system of equations:

$$\begin{aligned}
&\tilde{Q} - \hat{Q} = s \cdot (\tilde{\rho} - \hat{\rho}) \\
&\frac{\tilde{Q}^2}{\tilde{\rho}}(1+c) - \frac{\hat{Q}^2}{\hat{\rho}}(1+c) = s \cdot (\tilde{Q} - \hat{Q}) \ .
\end{aligned}$$

Writing down the solutions in terms of $\tilde{\rho}$ yields

$$\tilde{Q}_{1,2} = \hat{Q}\frac{1 \pm (\tilde{\rho} - \hat{\rho})\sqrt{\frac{c^2+c}{\tilde{\rho}\hat{\rho}}}}{1 - \frac{\tilde{\rho}-\hat{\rho}}{\tilde{\rho}}(1+c)} \tag{22}$$

and the corresponding shock speed

$$s_{1,2} = \hat{Q}\frac{\frac{1+c}{\tilde{\rho}} \pm \sqrt{\frac{c^2+c}{\tilde{\rho}\hat{\rho}}}}{1 - \frac{\tilde{\rho}-\hat{\rho}}{\tilde{\rho}}(1+c)} \ , \tag{23}$$

where the $\pm$ signs give two solutions, one for each family of characteristic fields.

Now let us see what sign we should choose in formula (22) for the 1-shock and for the 2-shock respectively. Since $\tilde{Q}$ can be expressed in terms of $\tilde{\rho}$, we can parametrize these curves by taking, e.g., $\tilde{\rho}_p(\xi;\hat{u}) = \hat{\rho} \cdot (\xi + 1)$ for $p = 1, 2$ with $\xi > -1$. Then from (22) and (23) we obtain:

$$\tilde{u}_p(\xi;\hat{u}) = \begin{bmatrix} \hat{\rho}(1+\xi) \\ \hat{Q}\frac{1 \pm \xi\sqrt{\frac{c^2+c}{\xi+1}}}{1 - \frac{\xi(c+1)}{\xi+1}} \end{bmatrix} \qquad s_p(\xi;\hat{u}) = \frac{\hat{Q}}{\hat{\rho}}\frac{\frac{1+c}{1+\xi} \pm \sqrt{\frac{c^2+c}{1+\xi}}}{1 - \frac{\xi(1+c)}{1+\xi}} \ .$$

The choice of sign for each family is determined by the behavior as $\xi \to 0$ where the following relations must hold (see (*11*) for details):

1. $\dfrac{\partial}{\partial \xi}\tilde{u}_p(0;\hat{u})$ is a scalar multiple of the eigenvector $r_p(\hat{u})$: so $\frac{\partial}{\partial \xi}\tilde{u}_p(0;\hat{u}) = \hat{\rho}\cdot r_p(\hat{u})$ in our case;
2. $s_p(0;\hat{u}) = \lambda_p(\hat{u})$ for $p = 1,\ 2$.

Using these relations we find that for the 1-shock we must choose the minus sign and for the 2-shock the plus sign.

Remark: We can see that each of the characteristic fields is *genuinely nonlinear*, which means that

$$\nabla^T \lambda_p(u)\cdot r_p(u) = c_p(c_p-1)\frac{Q}{\rho^2} \neq 0 \quad \text{for all } u = [\rho \ \ Q]^T \neq 0 \ ,$$

where

$$\nabla\lambda_p = \begin{bmatrix} \dfrac{\partial \lambda_p}{\partial \rho} \\ \dfrac{\partial \lambda_p}{\partial Q} \end{bmatrix}$$

is the gradient of λ_p $(p = 1, 2)$. $\Diamond$

Up to now, we have ignored the question of whether a given discontinuity is physically relevant. Lax (*10*) proposed an entropy condition to systems of equations that are genuinely nonlinear: the jump in the pth field (from state $\hat{u}$ to $\tilde{u}$) is admissible only if

$$\lambda_p(\hat{u}) > s > \lambda_p(\tilde{u}) \ ,$$

where s is the shock speed. Now suppose we connect $\hat{u}$ to $\tilde{u}$ by a 1-shock, then we get

$$c_1\frac{\hat{Q}}{\hat{\rho}} > s > c_1\frac{\tilde{Q}}{\tilde{\rho}} \ .$$

Replacing $s = \frac{\tilde{Q}-\hat{Q}}{\tilde{\rho}-\hat{\rho}}$ in the above inequality and using $c_1 = 1 + c - \sqrt{c^2+c}$, we obtain

$$\frac{\hat{Q}}{\hat{\rho}} - s + (c-\sqrt{c^2+c})\frac{\hat{Q}}{\hat{\rho}} > 0 > \frac{\tilde{Q}}{\tilde{\rho}} - s + (c-\sqrt{c^2+c})\frac{\tilde{Q}}{\tilde{\rho}} \ ,$$

which after few steps leads to

$$\begin{aligned} \frac{\hat{Q}\tilde{\rho}-\tilde{Q}\hat{\rho}}{\tilde{\rho}-\hat{\rho}} &< -\tilde{Q}(c-\sqrt{c^2+c}) \\ \frac{\hat{Q}\tilde{\rho}-\tilde{Q}\hat{\rho}}{\tilde{\rho}-\hat{\rho}} &> -\hat{Q}(c-\sqrt{c^2+c}) \ . \end{aligned}$$

Combining the last two inequalities we obtain

$$-\hat{Q}(c-\sqrt{c^2+c}) < -\tilde{Q}(c-\sqrt{c^2+c}) \quad \text{and thus} \quad \hat{Q} < \tilde{Q} \ .$$

So for the 1-shock we have obtained the following: $\hat{Q} < \tilde{Q}$, and we should take the minus sign in formulas (22) and (23). Combining these two conditions we can show that we must have $\tilde{\rho} > \hat{\rho}$.
Indeed, we distinguish two cases:

1. The denominator in (22) is positive: $1 - \frac{\tilde{\rho}-\hat{\rho}}{\tilde{\rho}}(1+c) > 0$. Hence, $\tilde{\rho} < \hat{\rho}(1+\frac{1}{c})$ and thus $\tilde{Q} = \hat{Q}\frac{1-(\tilde{\rho}-\hat{\rho})\sqrt{\frac{c^2+c}{\tilde{\rho}\hat{\rho}}}}{1-\frac{\tilde{\rho}-\hat{\rho}}{\tilde{\rho}}(1+c)} > \hat{Q}$ if and only if $(\tilde{\rho}-\hat{\rho})\sqrt{\frac{c^2+c}{\tilde{\rho}\hat{\rho}}} < \frac{\tilde{\rho}-\hat{\rho}}{\tilde{\rho}}(1+c)$ or $\tilde{\rho} > \hat{\rho}$, since for the inverse inequality we get a contradiction;
2. The denominator is negative: $1 - \frac{\tilde{\rho}-\hat{\rho}}{\tilde{\rho}}(1+c) < 0$, or $\tilde{\rho} > \hat{\rho}(1+\frac{1}{c}) > \hat{\rho}$, and thus $\tilde{\rho} > \hat{\rho}$, and we here can check that also $\tilde{Q} > \hat{Q}$ is satisfied.

In this way we obtain formulas (12)–(13) for a 1-shock wave.

5.2 Derivation of the formulas for the rarefaction waves

Let us compute $w(\cdot)$, using the fact that our model is genuinely nonlinear, as was shown in Section 5.1. Recall that (17) implies that ξ is an eigenvalue of $J(w(\xi))$. Differentiating $\xi = \lambda_p(w(\xi))$ w.r.t. ξ results in

$$1 = \nabla^T \lambda_p(w(\xi)) \cdot w'(\xi) = \nabla^T \lambda_p(w(\xi)) \cdot \alpha(\xi) \cdot r_p(w(\xi)) \ .$$

Hence,

$$\alpha(\xi) = \frac{1}{\nabla^T \lambda_p(w(\xi)) \cdot r_p(w(\xi))} \ ,$$

which results in the differential equation

$$w'(\xi) = \frac{r_p(w(\xi))}{\nabla^T \lambda_p(w(\xi)) \cdot r_p(w(\xi))} \quad \text{for } \xi_1 \le \xi \le \xi_2$$

with initial condition

$$w(\xi_1) = u_{\rm l},\ \xi_1 = \lambda_p(u_{\rm l}) < \xi_2 = \lambda_p(u_{\rm r}) \ .$$

For 1-rarefaction we have:

$$\lambda_1 = c_1\frac{Q}{\rho} = c_1 V, \quad r_1 = \begin{bmatrix} 1 & c_1\frac{Q}{\rho} \end{bmatrix}^T, \quad \nabla^T\lambda_1 \cdot r_1 = c_1(c_1-1)\frac{Q}{\rho^2} \neq 0 \ ,$$

and thus

$$\frac{d}{d\xi}\rho(\xi) = \frac{\rho^2(\xi)}{Q(\xi)} \cdot \frac{1}{c_1^2 - c_1} \qquad \text{with } \rho(\xi_1) = \rho_{\rm l} \tag{24}$$

$$\frac{d}{d\xi}Q(\xi) = \rho(\xi)\frac{1}{c_1 - 1} \qquad \text{with } Q(\xi_1) = Q_{\rm l},\ \xi_1 = \lambda_1(u_{\rm l}) = c_1\frac{Q_{\rm l}}{\rho_{\rm l}} \ , \tag{25}$$

which is a system of two ordinary nonlinear differential equations. We see that (24) can be written as

$$\frac{d}{d\xi}\left(\frac{1}{\rho}\right) = -\frac{1}{Q} \cdot \frac{1}{c_1^2 - c_1} \ .$$

Denoting $\eta = \frac{1}{\rho}$ we get the system

$$\begin{aligned} Q\,\frac{d\eta}{d\xi} &= -\frac{1}{c_1^2 - c_1} \\ \eta\,\frac{dQ}{d\xi} &= \frac{1}{c_1 - 1} \ . \end{aligned}$$

We add both equations obtaining a relation between states: $Q(\xi) = \frac{1}{c_1}\xi\rho(\xi)$, and finally after some computations we obtain the following solution:

$$\rho(\xi) = \left(\frac{\rho_{\rm l}^{c_1}}{c_1 Q_{\rm l}} \cdot \xi\right)^{\frac{1}{c_1-1}}$$
$$Q(\xi) = \frac{\xi}{c_1}\left(\frac{\rho_{\rm l}^{c_1}}{c_1 Q_{\rm l}} \cdot \xi\right)^{\frac{1}{c_1-1}} \quad .$$

If we want to obtain an explicit expression for the integral curves in the phase plane, we eliminate ξ:

$$\rho^{c_1-1} = \xi \cdot \frac{\rho_{\rm l}^{c_1}}{c_1 Q_{\rm l}} \quad \Rightarrow \quad \xi = \frac{c_1 Q_{\rm l}}{\rho_{\rm l}^{c_1}}\rho^{c_1-1} \quad \Rightarrow \quad Q(\rho) = Q_{\rm l}\left(\frac{\rho}{\rho_{\rm l}}\right)^{c_1} \quad .$$

We can construct the 2-rarefaction wave in exactly the same manner obtaining

$$\rho(\xi) = \left(\frac{\rho_{\rm l}^{c_2}}{c_2 Q_{\rm l}} \cdot \xi\right)^{\frac{1}{c_2-1}}$$
$$Q(\xi) = \frac{\xi}{c_2}\left(\frac{\rho_{\rm l}^{c_2}}{c_2 Q_{\rm l}} \cdot \xi\right)^{\frac{1}{c_2-1}} \quad ,$$

and in the phase plane 2-rarefaction is given by

$$Q(\rho) = Q_{\rm l}\left(\frac{\rho}{\rho_{\rm l}}\right)^{c_2} \quad .$$

Now two states $u_{\rm l}$ and $u_{\rm r}$ can be connected by a rarefaction wave provided that they lie on the same integral curve and $\lambda_p(u_{\rm l}) < \lambda_p(u_{\rm r})$, which for 1-rarefaction results in

$$c_1 \cdot \frac{Q_{\rm l}}{\rho_{\rm l}} < c_1 \cdot \frac{Q_{\rm r}}{\rho_{\rm r}}, \qquad c_1 \in (0,1) \ ,$$

with

$$Q_{\rm r} = Q_{\rm l}\left(\frac{\rho_{\rm r}}{\rho_{\rm l}}\right)^{c_1} \quad ,$$

and thus

$$\frac{1}{\rho_{\rm l}} < \frac{\rho_{\rm r}^{c_1-1}}{\rho_{\rm l}^{c_1}} \quad .$$

Hence, $\rho_{\rm l}^{c_1-1} < \rho_{\rm r}^{c_1-1}$ or $\rho_{\rm r} < \rho_{\rm l}$ since $c_1 \in (0,1)$. Therefore, a 1-rarefaction wave is indeed described by (18). Similarly, we can show that a 2-rarefaction wave is described by (19).

6 CONCLUSIONS AND FUTURE RESEARCH

In this paper we have discussed some properties of Helbing's traffic flow model. More specifically, we have derived the formulas for shocks and rarefaction waves. By selecting the states that satisfy the Lax entropy condition, we saw that we cannot connect to negative states. Finally, we have considered the Riemann problem associated with the Helbing model, based on the results in connection with the shocks and rarefaction waves. In particular, we have proved that when we have a Riemann problem with non-negative densities and flows on either side of discontinuity in the initial condition, the Helbing model cannot give rise to negative flows and density later on.

Topics for further research include: investigation of appropriate efficient numerical schemes to simulate this model (in particular, to further characterize and investigate the jump and wave phenomena considered in this paper, and also for on-line simulation), and extension of the results to other continuum models (such as Hoogendoorn's model (*8*)).

ACKNOWLEDGMENTS

The authors would like to thank the anonymous reviewers for their careful review and their extensive feedback with useful additions and suggestions for improvement, which certainly contributed to improving the clarity of this paper.

Research supported by the NWO-CONNEKT project "Advanced multi-agent control and information for integrated multi-class traffic networks", the STW project "Multi-agent control of large-scale hybrid systems", and the TU Delft Spearhead Program "Towards Reliable Mobility".

REFERENCES

[1] R. Ansorge. What does the entropy condition mean in traffic flow theory. *Transportation Research Part B*, 24(2):133–143, 1990.

[2] C.F. Daganzo. Requiem for second-order fluid approximations of traffic flow. *Transportation Research Part B*, 29(4):277–286, August 1995.

[3] J.M. del Castillo. A formulation for the reaction time of traffic flow models. In C. Daganzo, editor, *Transportation and Traffic Theory*, pages 387–405, 1993.

[4] D. Helbing. High-fidelity macroscopic traffic equations. *Physica A*, 219:391–407, 1995.

[5] D. Helbing. Derivation and empirical validation of a refined traffic flow model. *Physica A*, 233:253–282, 1996.

[6] D. Helbing. Derivation, properties, and simulation of a gas-kinetic-based, nonlocal traffic model. *Physical Review E*, 59(1):239–253, 1999.

[7] D. Helbing. Micro- and macro-simulation of freeway traffic. *Mathematical and Computer Modelling*, 35:517–547, 2002.

[8] S.P. Hoogendoorn and P.H.L. Bovy. Generic gas-kinetic traffic systems modeling with applications to vehicular traffic flow. *Transportation Research Part B*, 35(4):317–336, May 2001.

[9] B.S. Kerner and P. Konhauser. Structure and parameters of clusters in traffic flow. *Physical Review E*, 50(1), 1994.

[10] P.D. Lax. *Hyperbolic Systems of Conservation Laws and the Mathematical Theory of Shock Waves*. Society for Industrial and Applied Mathematics, Philadelphia, PA, 1973.

[11] R.J. LeVeque. *Numerical Methods for Conservation Laws*. Lectures in Mathematics. Birkhauser, 1992.

[12] M.J. Lighthill and G.B. Whitham. On kinematic waves: II. A theory of traffic flow on long crowded roads. *Proceedings of the Royal Society of London*, 299A:317–345, May 1955.

[13] S. Osher. Riemann solvers, the entropy condition and difference approximation. *SIAM Journal on Numerical Analysis*, 21:217–235, 1984.

[14] S.L. Paveri-Fontana. On Boltzmann-like treatments for traffic flow. A critical review of the basic model and an alternative proposal for dilute traffic analysis. *Transportation Research*, 9:225–235, 1975.

[15] H.J. Payne. Models of freeway traffic and control. In G.A. Bekey, editor, *Mathematical Models of Public Systems*, volume 1, no. 1 of *Simulation Council Proceedings Series*, pages 51–61. La Jolla, California, 1971.

[16] I. Prigogine and R. Hermann. *Kinetic Theory Of Vehicular Traffic*. Elsevier, New York, 1971.

[17] P.I. Richards. Shock waves on the highway. *Operations Research*, 4:42–51, 1956.

[18] E.F. Toro. *Riemann Solvers and Numerical Methods for Fluid Dynamics — A Practical Introduction*. Springer Verlag, 2nd edition, 1999.

[19] G.B. Whitham. *Linear and Nonlinear Waves*. Wiley, New York, 1974.

[20] H.M. Zhang. Structural properties of solutions arising from a nonequilibrium traffic flow theory. *Transportation Research Part B*, 34:583–603, 2000.

LIST OF FIGURES

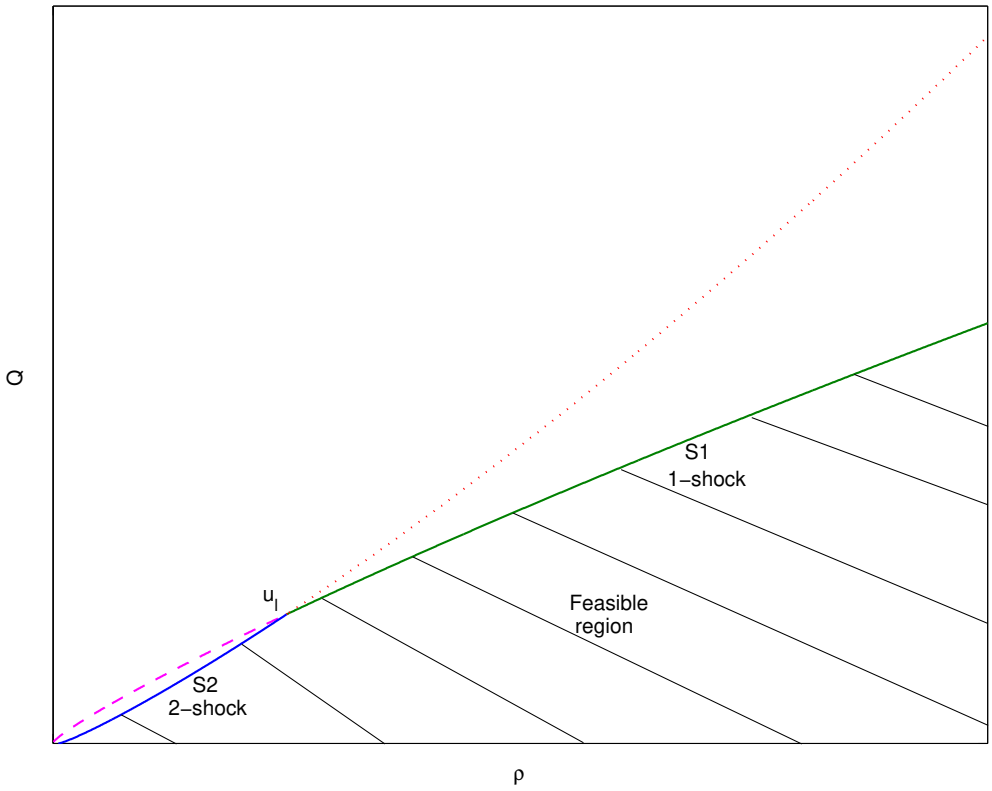

FIGURE 1 Representation of the states u_{r} that can be connected to u_{l} by an entropy-satisfying shock. State u_{r} can be connected to u_{l} by a 1-shock if u_{r} lies on curve S1 passing through u_{l}, and by a 2-shock if u_{r} lies on curve S2 passing through u_{l}. The dotted and dashed curves represent entropy-violating points.

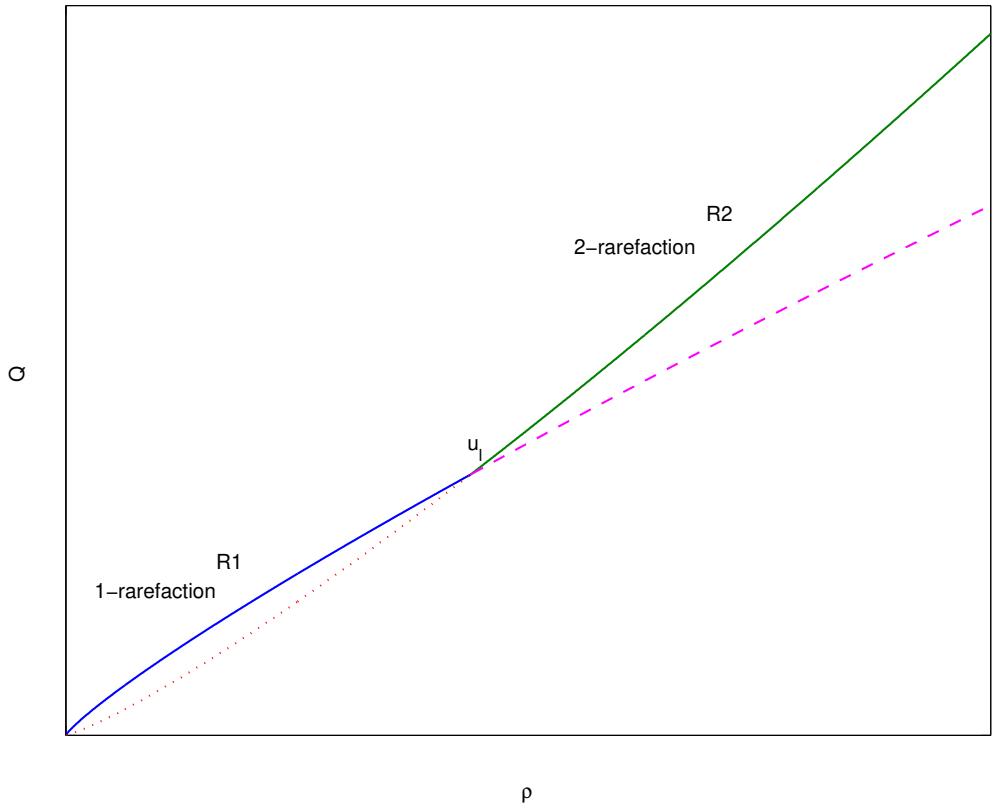

FIGURE 2 Representation of the states u_{r} that can be connected to u_{l} by a rarefaction wave. State u_{r} can be connected to u_{l} by a 1-rarefaction if u_{r} lies on curve R1 passing through u_{l}, and by a 2-rarefaction wave if u_{r} lies on curve R2 passing through u_{l}. The dotted and dashed curves represent points that do not satisfy the rarefaction condition (14).

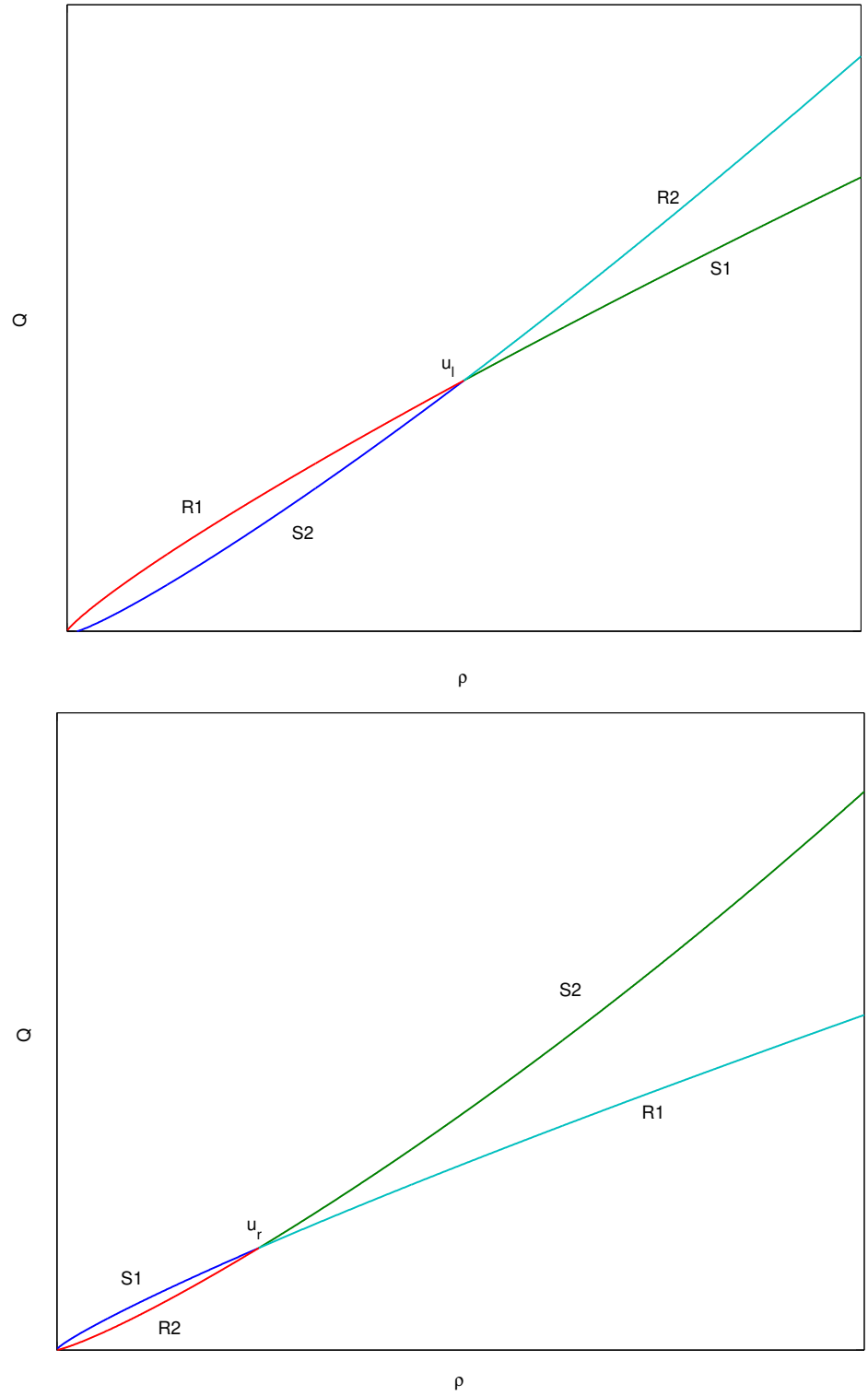

FIGURE 3 Representation of the states u_{r} that can be connected to u_{l} by a shock or a rarefaction wave (top), and of the states u_{l} that can be connected to u_{r} by a shock or a rarefaction wave (bottom).

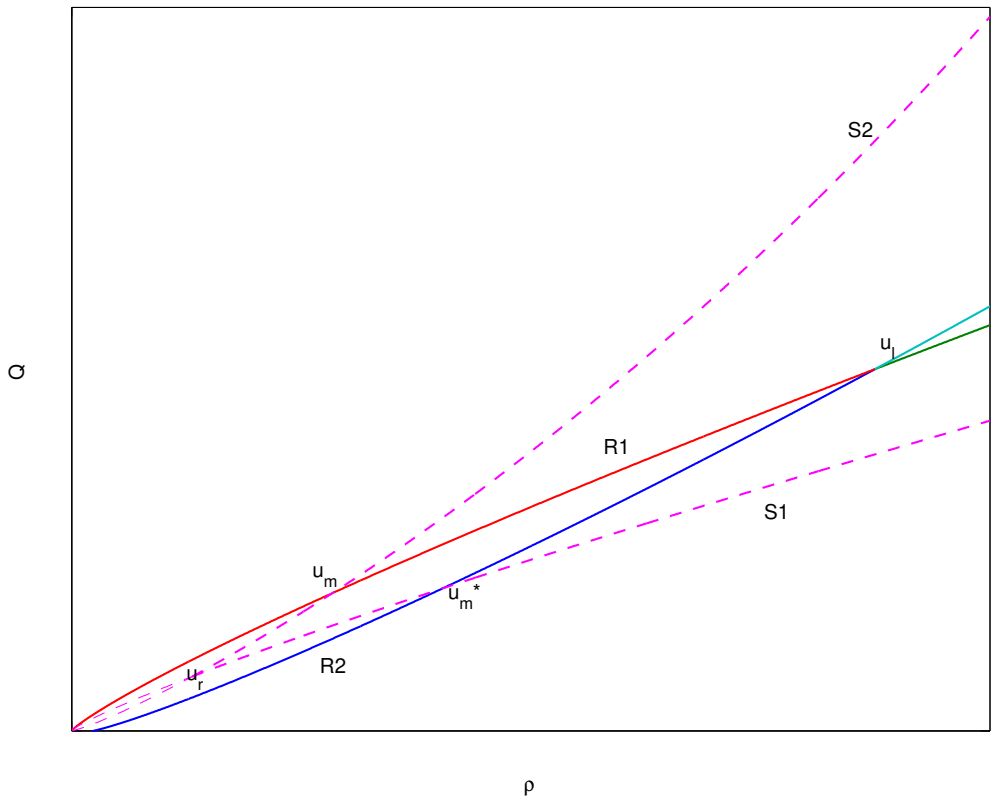

FIGURE 4 Construction of the solution for the Riemann problem. We obtain two intermediate states u_{m} and u_{m}^*, but only u_{m}^* is a physically valid solution.